Renewable and Sustainable Energy Reviews 16 (2012) 2118–2132

Contents lists available at SciVerse ScienceDirect

Renewable and Sustainable Energy Reviews

journal homepage: www.elsevier.com/locate/rser

Review on storage materials and thermal performance enhancement techniques for high temperature phase change thermal storage systems

Ming Liu*, Wasim Saman, Frank Bruno

Barbara Hardy Institute, University of South Australia, Mawson Lakes, SA 5095, Australia

ARTICLE INFO

Article history:
Received 25 August 2011
Accepted 5 January 2012
Available online 18 February 2012

Keywords:
Phase change materials
Latent heat thermal energy storage
Heat transfer rate
Thermal performance enhancement
High temperature thermal energy storage

ABSTRACT

Designing a cost-effective phase change thermal storage system involves two challenging aspects: one is to select a suitable storage material and the other is to increase the heat transfer between the storage material and the heat transfer fluid as the performance of the system is limited by the poor thermal conductivity of the latent heat storage material. When used for storing energy in concentrated solar thermal power plants, the solar field operation temperature will determine the PCM melting temperature selection. This paper reviews concentrated solar thermal power plants that are currently operating and under construction. It also reviews phase change materials with melting temperatures above 300 °C, which potentially can be used as energy storage media in these plants. In addition, various techniques employed to enhance the thermal performance of high temperature phase change thermal storage systems have been reviewed and discussed. This review aims to provide the necessary information for further research in the development of cost-effective high temperature phase change thermal storage systems.
© 2012 Elsevier Ltd. All rights reserved.

Contents

1. Introduction 2118
2. Thermal energy storage employed in solar power plants 2119
3. High temperature phase change materials 2119
   3.1. Inorganic salts and salt composites 2119
   3.2. Metals and metal alloys 2123
4. Methods of performance enhancement 2124
   4.1. Enhancement using high conductive materials 2124
   4.2. Enhancement using extended heat transfer surface 2126
   4.3. Enhancement using intermediate heat transfer medium 2127
   4.4. Enhancement using heat pipes 2128
   4.5. Enhancement using multiple PCMs 2129
5. Conclusions and discussions 2130
   Acknowledgement 2131
   References 2131

1. Introduction

Solar thermal energy is taking up increasing proportions of future power generation worldwide. The number of solar thermal power plants completed and under construction in Southern Europe, USA, Africa and Australia is increasing as a means for generating electricity by replacing conventional steam boilers in power plants with high temperature solar collecting devices. Thermal energy storage technology solves the time mismatch between solar energy supply and electricity demand. However, there is currently no available cost-effective compact storage technology according to the International Energy Agency (IEA) Task 42/24 (http://www.iea-shc.org/task42/index.html). The state of the art thermal energy storage systems are sensible heat storage in cold and hot molten salt tanks. These require expensive, unwieldy tanks and large volumes of storage materials. For example, the Andasol I solar power plant located in Spain is capable of producing 50 MWe electricity. The storage system consists of two

* Corresponding author. Tel.: +61 08 83025132; fax: +61 08 83023380.
E-mail address: ming.liu@unisa.edu.au (M. Liu).

1364-0321/$ – see front matter © 2012 Elsevier Ltd. All rights reserved.
doi:10.1016/j.rser.2012.01.020

molten salt storage tanks measuring 14 m in height and 36 m in diameter.

Compared to sensible heat storage, phase change materials (PCMs) allow large amounts of energy to be stored in relatively small volumes, resulting in some of the lowest storage media costs of any storage concepts [1]. PCM is a substance with a high heat of fusion which, melting and solidifying at certain temperatures, is capable of storing or releasing large amounts of latent energy. When solar radiation is available, the heat energy obtained from the solar receiver can be stored in the PCM by changing the phase of the PCM from solid to liquid, which is called the charging process. Later on, when there is higher electricity demand or tariffs or during cloudy periods, the stored heat can be recovered and used for steam generation. During the discharging process, the PCM freezes.

Due to the advantages offered by latent heat thermal energy storage, such as low temperature variation during charging and discharging cycles, small unit size, high storage density and relatively constant heat transfer fluid (HTF) temperature during the discharge process, it has been applied into numerous low temperature applications including solar heating and cooling systems [2–6], conventional air-conditioning system [7–9], refrigeration system [10], underfloor heating system [11–13], building envelope [14–16] and solar cooker [17–19]. Various studies [20–23] gave detailed illustrations about their classification, characteristics, measurement techniques and their benefits and limitations. However, most PCMs have low thermal conductivity around 0.5 W/(m K), which leads to the poor heat transfer between the HTF and the PCM [24] and hence limits the application of latent thermal storage technology in practical systems.

A number of desirable properties for choosing PCMs have been proposed by Abhat [20] and Lane [25] considering thermodynamic, kinetic, chemical and economic aspects. These properties include:

- A demanded melting/freezing temperature, which should be within the desired usage temperature range.
- High values of specific heat, latent heat of fusion and density to provide the minimum size of the thermal storage unit. Also, a small variation in density between solid and liquid phases is desired, which will enable the choice of a simple containment and heat exchange component.
- A high thermal conductivity to provide high heat transfer rates into and out of PCMs.
- Congruent melting. The material should melt congruently, otherwise, it will result in irreversible segregation of components.
- Insignificant supercooling as the supercooling will reduce the heat storage capacity of PCMs.
- Chemical stability to provide a reasonable life time of storage unit.
- Non corrosive to containment materials, non-poisonous, non-flammable and non-explosive.
- Abundant supply and at a low cost.

This paper reviews the available PCMs and materials with potential use as PCMs with melting temperatures above 300 °C, which can be employed to store the heat obtained from high temperature concentrated solar thermal power plants. Also, various thermal performance enhancement techniques employed on high temperature phase change thermal storage systems are reported. These techniques include improving the thermal conductivity of the PCM by high conductive materials, extending heat transfer surfaces, using intermediate heat transfer medium, using heat pipes and employing multiple PCMs.

2. Thermal energy storage employed in solar power plants

Before selecting the high temperature PCMs, the storage temperature and solar field working temperature in concentrated solar thermal power plants are reviewed as they determine the melting temperature range of the PCM. Concentrated solar thermal power plants can be classified into four configurations: linear fresnel, parabolic trough, central receiver tower and dish. Table 1 lists the currently operated and under-construction concentrated solar thermal power plants. The information is summarised from a project listing hosted by the National Renewable Energy Laboratory (NREL) at http://www.nrel.gov/csp/solarpaces/ and references [26,27]. It provides detailed information on the thermal energy storage systems, such as whether the power plant incorporates a storage system, storage concept, storage capacity, storage medium and storage temperature.

It can be seen from Table 1 that parabolic troughs, which are the most mature concentrated solar thermal power technology, form most of the currently available commercial solar power plants. A majority of plants in operation have thermal storage capacity to increase the system reliability and generation capacity. The state of the art thermal storage system is the two-tank active indirect storage employing molten salts (60% $NaNO_3$ and 40% KNO_3) as the storage material and synthetic oil as the HTF. The storage and solar field temperatures are in the range of around 300–400 °C as the synthetic oil has an upper temperature limit of 400 °C. It should be noted that the Archimede solar power plant in Italy is the first using molten salt as the HTF and the solar field outlet temperature is increased to 550 °C. It is known that high HTF operating temperatures generally allow for higher temperature storage, which results in higher efficiency thermal storage and higher turbine efficiency.

3. High temperature phase change materials

High temperature PCMs with melting temperatures above 300 °C, which have the potential for thermal energy storage in concentrated solar power plants, are reviewed. They include pure salts, salt eutectics, metals and metal eutectics. Among them, the PCMs having melting temperatures in the range of 300–550 °C can be potentially employed as energy storage media for solar power plants with currently available HTFs (oils, water/steam and molten salts). Alternative HTFs (e.g. supercritical CO_2 and other molten salts) are under investigation by research teams worldwide. Therefore, higher operation temperatures are achievable and higher storage temperatures (above 550 °C) may be required in the future.

3.1. Inorganic salts and salt composites

Tables 2 and 3 present the pure inorganic salts and salt composites that have been investigated by different researchers for their potential use as high temperature PCMs above 300 °C. Some of their thermophysical properties are included, such as melting temperature, latent heat of fusion, density, specific heat and thermal conductivity. Some references give thermal expansion coefficient during phase change. It should be noted that only the pure salt based on chlorides, sulphates, nitrates and carbonates are chosen in Table 2 due to their availability and low cost.

Zalba et al. [21] comprehensively reviewed potential PCMs with melting temperatures up to 900 °C. They include inorganic substances, inorganic eutectics, non-eutectic mixtures of inorganic substances, organic substances and organic eutectics. In Kenisarin's review paper [28], he listed hundreds of inorganic salts and salt composites for latent heat storage in the temperature range from 120 to 1000 °C. Those storage materials are on the basis of fluorides, chlorides, bromides, hydroxides, nitrates, carbonates and other salts. He found out that only a limited number of pure inorganic salts possess decent latent heat of fusion. Double and ternary eutectic compositions based on fluorides and chlorides are the most

Table 1
Existing and under-construction concentrated solar thermal power plants & their thermal energy storage systems.

Project and location	Total capacity (MWe)	Technology type	HTF in solar field	Storage concept	Storage capacity (MWh)	Storage material	Storage temperature		Solar field temperature (°C)		Operational/under construction
							Cold (°C)	Hot (°C)	Inlet (°C)	Outlet (°C)	
SEGS I-IX Mojave Desert, California, USA	354	Parabolic trough	Mineral oil (SEGS I) synthetic oil (SEGS II-IX)	Two-tank active direct (SEGS I)	120 (SEGS I)	Mineral oil (SEGS I)	240	307	–	SEGS I: 307 SEGS II: 316 SEGS III-V: 349 SEGS VI-IX: 391	O
Solnova Seville, Spain	250 (5 × 50)	Parabolic trough	Thermal oil	–	–	–	–	–	–	393	O
Andasol Andalusia, Spain	200 (4 × 50)	Parabolic trough	Synthetic oil	Two-tank active indirect	1010	28,500 tons molten salt	291	384	293	393	Andasol 1 and 2: O Andasol 3 and 4: U
Extresol Torre de Miguel Sesmero, Spain	100 (2 × 50)	Parabolic trough	Synthetic oil	Two-tank active indirect	1010	28,500 tons molten salt	–	–	293	393	O
Helio Arenas de San Juan, Spain	100 (2 × 50)	Parabolic trough	–	–	–	–	–	–	–	–	U
Palma del Río Palma del Río, Spain	100 (2 × 50)	Parabolic trough	Synthetic oil	–	–	–	–	–	318	393	U
Nevada Solar One Boulder City, Nevada, USA	64	Parabolic trough	Synthetic oil	n.a.	0.5 h full-load storage	n.a.	n.a.	n.a.	318	391	O
Puertollano Puertollano, Spain	50	Parabolic trough	Synthetic oil	–	–	–	–	–	304	391	O
Alvarado I Alvarado, Spain	50	Parabolic trough	Synthetic oil	–	–	–	–	–	–	393	O
Arcosol 50 San José del Valle, Spain	50	Parabolic trough	Synthetic oil	Two-tank active indirect	1010	28,500 tons molten salt	–	–	293	393	U
Lebrija I Lebrija, Spain	50	Parabolic trough	Therminol VP1 (Synthetic oil)	–	–	–	–	–	–	395	U
La Florida Badajoz, Spain	50	Parabolic trough	Synthetic oil	Two-tank active indirect	1010	29,000 tons molten salt	–	–	298	393	O
El Reboso II Sevilla, Spain	50	Parabolic trough	Synthetic oil	–	–	–	–	–	296	393	U
El Reboso III Sevilla, Spain	50	Parabolic trough	Synthetic oil	Two-tank active indirect	116	Molten salt	–	–	296	393	U
La Dehesa La Garrovilla, Spain	50	Parabolic trough	Synthetic oil	Two-tank active indirect	1010	29,000 tons molten salt	–	–	298	393	O
Majadas I Majadas de Tiétar, Spain	50	Parabolic trough	Synthetic oil	–	–	–	–	–	–	393	O
Manchasol-1 Alcazar de San Juan, Spain	50	Parabolic trough	Synthetic oil	Two-tank active indirect	375	28,500 tons molten salt	–	–	293	393	O
Archimede Sicily, Italy	5	Parabolic trough	Molten salt	Two-tank active direct	100	1580 tons molten salt	–	–	290	550	O
Kimberlina Bakersfeild, California, USA	5	Linear Fresnel	Water	–	–	–	–	–	–	–	O
Puerto Errado 1 Calasparra, Spain	1.4	Linear Fresnel	Water	Single-tank (thermocline)	–	–	–	–	140	270	O
Puerto Errado 2 Calasparra, Spain	30	Linear Fresnel	Water	Single-tank (thermocline)	–	–	–	–	140	270	U
Liddell New South Wales, Australia	2	Linear Fresnel	Water	–	–	–	–	–	–	–	O
Ivanpah Primm, NV, California, USA	392	Power Tower	Water	–	–	–	–	–	250	565	U
Gemasolar (Solar Tres) Fuentes de Andalucía, Spain	15	Power Tower	Molten salt	Two-tank active direct	600	6250 tons Molten salt	290	565	290	565	U
Planta Solar 10 Sevilla, Spain	11	Power Tower	Water	Active direct	20	Pressured water	285 °C, 50 bar	–	250–300 °C	O	
Planta Solar 20 Sevilla, Spain	20	Power Tower	Water	Active direct	–	Steam-ceramic	–	–	–	250–300 °C	O
Sierra Lancaster, California, USA	5	Power Tower	Water	–	–	–	–	–	218	440	O
Maricopa Peoria, Arizona	1.5	Dish/Engine	–	–	–	–	–	–	–	–	O

Note: "–" in the table means the information is not available.

Table 2
Inorganic substances with potential use as PCM.

Compound	Melting temperature (°C)	Heat of fusion (kJ kg^{-1})	Density (kg/m^3)		Specific heat (kJ kg^{-1} K)		Thermal conductivity (W/m K)		Thermal expansion coefficient (K^{-1})	References	Note
			Solid	Liquid	Solid	Liquid	Solid	Liquid			
$NaNO_3$	306	172	2261		1.10		0.5			[69]	168 cycles in test module shows no decomposition
	306	175			1.5	1.7				[38]	172 cycles in test module shows no change in T_m
	306	178	2260 @ 25 °C	1908 @ 306 °C		1.655 @306 °C		0.514 @306 °C	40×10^{-6}	[37]	2600 h oven test
	306	175	1900							[40]	
	308	200	2257		0.5		[27]				
	310	174					[74]				
	310	172	2260	1.82	0.5		[52]				
NaOH	318	165	2100	2.08	0.92		[52]				
	320	159	1785	2.15			[32]				
KNO_3	335	95	2109		0.953		0.5	0.425	200×10^{-6}	[62,69]	
	333	267	2110		0.5		[27]				
	330	266	2110	1.22	0.5		[52]				
KOH	360	134	2040		1.34		0.5			[69]	
	380	150	2044	1.47	0.5		[27,52]				
$Mg(NO_3)_2$	426						[28]				
$Ca(NO_3)_2$	560	145					[28]				
$MgCl_2$	714	452	2140				[75]				
KCl	771	353					[28]				
NaCl	802	420	2160		5.0		[27]				
	800	482					[43]				
	800	481					[61]				
Na_2CO_3	854	276	2533		2.0		[27]				
Na_2SO_4	884	165					[28]				
K_2CO_3	897	236	2290		2.0		[27]				

Table 3
Inorganic eutectics with potential use as PCM.

Compound (wt%)	Melting temperature (°C)	Heat of fusion ($kJ\,kg^{-1}$)	Density (kg/m^3)		Specific heat ($kJ\,kg^{-1}\,K$)		Thermal conductivity (W/m K)		Thermal expansion coefficient (K^{-1})	References	Note
			Solid	Liquid	Solid	Liquid	Solid	Liquid			
LiOH/KOH (40/60)	314	341								[74]	
KNO_3/KCl (95.5/4.5)	320	74	2100		1.21		0.5			[69]	
KNO_3/KCl (96/4)	320	150								[74]	
KNO3/KBr/KCl (80/10/10)	342	140								[74]	
NaCl/KCl/LiCl (33/24/43)	346	281								[74]	
NaOH/NaCl (80/20)	370	370								[74]	
$MgCl_2$/KCl/NaCl (60/20.4/19.6)	380	400	1800		0.96					[69]	
Li_2CO_3/K_2CO_3/Na_2CO_3 (32.1/34.5/33.4)	397	276								[33]	50 thermal cycles
$MgCl_2$/KCl (39/61)	435	351	2110		0.80	0.96		0.81		[28]	
$MgCl_2$/NaCl (52/48)	450	430	2230		0.92	1.00		0.95		[28]	
$MgCl_2$/KCl (64/36)	470	388	2190		0.84	0.96		0.83		[28]	
$MgCl_2$/KCl/$CaCl_2$ (48/25/27)	487	342	2530		0.80	0.92		0.88		[28]	
$CaCl_2$/NaCl (67/33)	500	281	2160		0.84	1.00		1.02		[28]	
NaCl/KCl/$CaCl_2$ (29/5/66)	504	279	2150		1.17	1.00		1.00		[28]	
$BaCl_2$/KCl/NaCl (53/28/19)	542	221	3020		0.63	0.80		0.86		[28]	
$BaCl_2$/KCl/$CaCl_2$ (47/24/29)	551	219	2930		0.67	0.84		0.95		[28]	
LiF/MgF_2/KF (64/30/6 mol%)	710	782					[34]				
LiF/CaF_2 (80.5/19.5 mol%)	767	790					[35,36]				

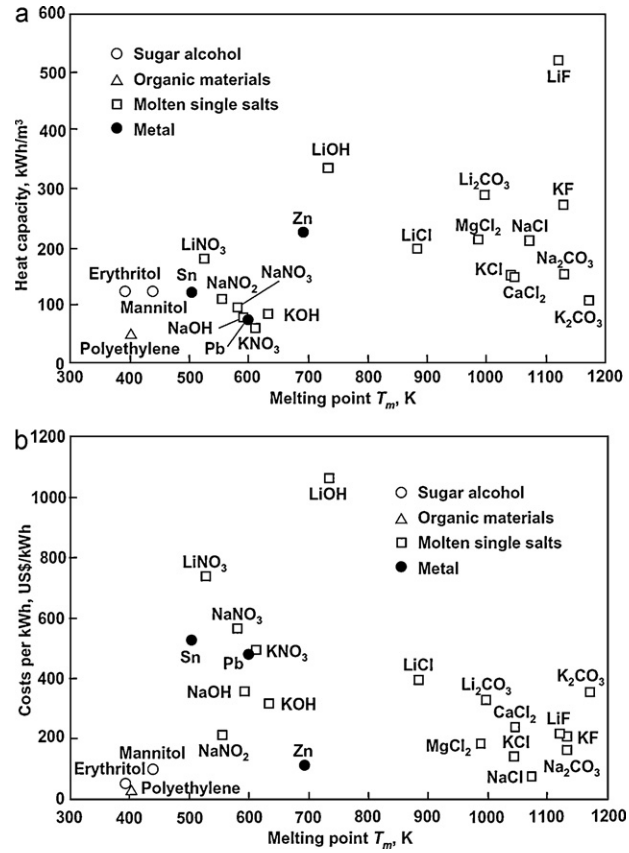


Fig. 1. Heat capacity (a) and media cost (b) of high melting point PCMs [29].

prospective PCMs in term of their high latent heat of fusion and also the low cost of the latter. Hoshi et al. [29] reviewed the potential PCMs with melting temperatures up to 900 °C. The heat capacity and media cost were plotted against the melting point of the PCM as shown in Fig. 1(a) and (b). For the melting temperature range of interest here, $NaNO_3$, NaOH, KNO_3, KOH, LiCl, Pb and Zn may be used as PCMs, among which, KOH and Zn seem the most cost effective salt and metal.

A numerical model was developed by Elgafy et al. [30] to predict the thermal performance of a high melting point PCM during its melting and solidification processes within a cylindrical enclosure. They verified the model using a PCM with a high latent heat of fusion (1043.6 $kJ\,kg^{-1}$) and thermal conductivity (14.2 $W\,m^{-1}\,K^{-1}$). Nomura et al. [31] examined the use of an eutectic mixture of NaOH/Na_2CO_3 as a PCM in waste-heat transportation system. Differential scanning calorimeter (DSC) analysis showed that its thermophysical properties are stable after aging for 500 h during phase change. A PCM (NaOH) was selected to recover the waste heat due to its large latent heat during solid–solid transformation at 293 °C (159 $kJ\,kg^{-1}$) and solid–liquid phase change at 320 °C (159 $kJ\,kg^{-1}$) [32].

Generally, fluoride salts have high heat storage capacity, but they become less attractive in terms of cost and materials compatibility [33]. Ponnappan and Jacobson [34] tested a ternary fluoride eutectic salt (LiF/MgF_2/KF: 64/30/6 wt%) filled in a cylindrical container in a calorimeter system. The measured latent heat of fusion was very high, being 782.26 $kJ\,kg^{-1}$. Another inorganic eutectic having a very high latent heat of fusion is LiF/CaF_2 (80.5/19.5 wt%). The value is 790 $kJ\,kg^{-1}$ [35,36].

Shin et al. [33] tested a salt eutectic (Li_2CO_3/K_2CO_3/Na_2CO_3: 32.1/34.5/33.4 wt%) with a weight of 3.8 kg in the experimental apparatus as shown in Fig. 2. The eutectic exhibits a distinct

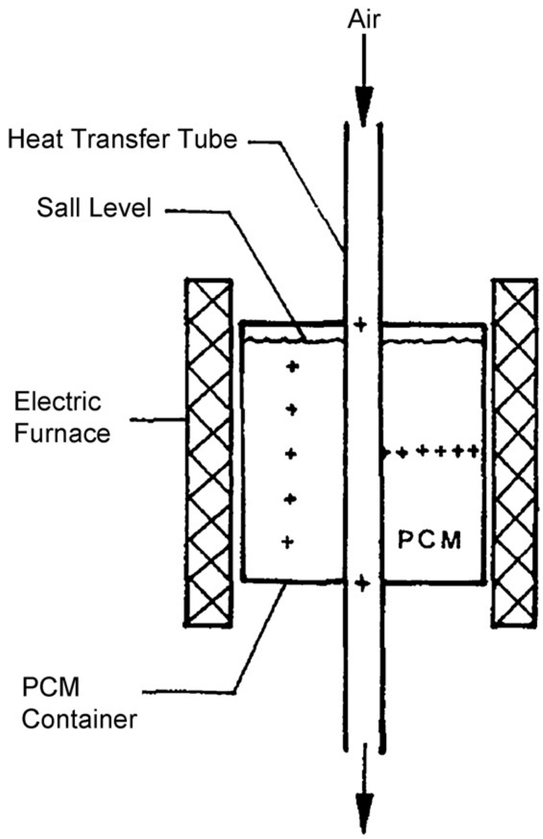


Fig. 2. Schematic diagram of the experimental apparatus testing the ternary carbonate eutectic mixture [33].



Fig. 3. $NaNO_3$ storage prototype [40].

phase change temperature (395–397 °C) without phase separation or supercooling over 50 thermal cycles.

The German Aerospace Centre (DLR) did intensive research to investigate sodium nitrate ($NaNO_3$) as a PCM. $NaNO_3$ is the most suitable candidate to generate steam at a pressure of around 100 bar in direct steam generation technology. Bauer et al. [37] experimentally examined the thermal stability and thermophysical properties of $NaNO_3$, which are listed in Table 2. In the thermal stability test, the salt was heated in a borosilicate glass beaker and placed in a batch furnace at 350 °C for 2600 h. The results showed that $NaNO_3$ is thermally stable at 350 °C and a small amount of nitrate is formed. Also, the compatibility study on molten $NaNO_3$ and graphite foil showed the molten $NaNO_3$ oxidizes graphite. Laing et al. [38] tested a prototype storage unit (Fig. 3) with aluminium fins (Fig. 4) filled with 140 kg of sodium nitrate. The operation of 172 cycles (more than 4000 h) proved no decomposition of the PCM and no degradation of fins. Then the storage module was scaled up to around 14 tons of $NaNO_3$. A photo of this PCM module is shown in Fig. 5. The PCM module combining with two concrete sensible storage modules will be tested in a direct steam generation test facility in Spain under real steam conditions [39]. The two concrete storage modules are used to store the heat for preheating and superheating the water/steam.

3.2. Metals and metal alloys

Some problems of inorganic salts and salt composites limit their applications, such as low thermal conductivity, high corrosion and large volume changes during melting. Metals diminish these problems and are quite competitive despite the lower density of the heat storage. Table 4 lists the metals and metal alloys with melting temperatures above 300 °C. Farkas and Birchenall [40] and Gasanealiev and Gamataeva [41] reported many binary and ternary metallic eutectic alloys with melting temperatures above 300 °C. Akiyama et al. [42] analyzed the thermal performance of spherical capsules containing six PCMs during heat storage and heat release processes respectively. The PCMs under investigation include salt/salt eutectic (NaCl, $NaNO_3/KNO_3$) and metals/metal alloys (Pb, Al, Al/Si: 12.6/87.4 wt% and Al/Si: 25.1/74.9 wt%). The result shows that metallic PCMs are more advantageous for the purpose of obtaining constant temperature HTF because of higher thermal conductivity. Al–Si alloys with 12 wt% Al and 20 wt% Al were tested respectively using a DSC [43]. Their melting temperatures and heats of fusion are listed in Table 4. Due to a higher latent heat of fusion of Al–Si alloy with 12 wt% Al, it has been selected for

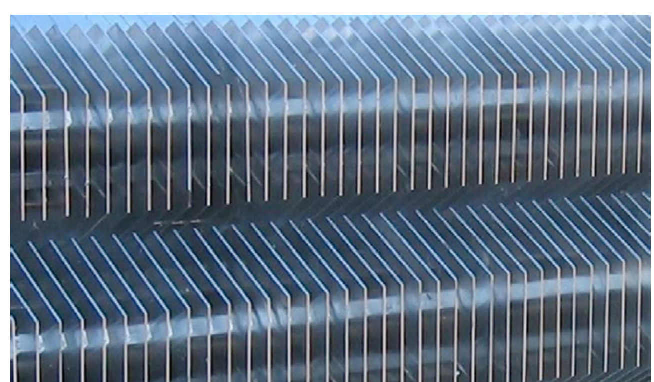


Fig. 4. Fins for heat transfer enhancement [40].

Table 4
Metals and metal alloys with potential use as PCM.

Compound	Melting temperature (°C)	Heat of fusion ($kJ\,kg^{-1}$)	Density (kg/m^3)		Specific heat ($kJ\,kg^{-1}\,K$)		Thermal conductivity (W/m K)		References	Note
			Solid	Liquid	Solid	Liquid	Solid	Liquid		
Pb	328	23							[43]	
Al	660	397							[43]	
Cu	1083	193.4	8930						[76]	
			8800				350		[40]	
Mg–Zn (46.3/53.7 wt%)	340	185	4600						[42]	
Mg–Zn (48/52 wt%)	340	180							[41]	
Zn–Al (96/4 wt%)	381	138	6630						[42]	
Al–Mg–Zn (59/33/6 wt%)	443	310	2380		1.63	1.46			[41]	
Al–Mg–Zn (60/34/6 wt%)	450.3	329.1							[45]	1000 thermal cycles
Mg–Cu–Zn (60/25/15 wt%)	452	254	2800						[41]	
Mg–Cu–Ca (52/25/23 wt%)	453	184	2000						[41]	
Mg–Al (34.65/65.35 wt%)	497	285	2155						[42]	
Al–Cu–Mg (60.8/33.2/6 wt%)	506	365	3050						[42]	
Al–Si–Cu–Mg (64.6/5.2/28/2.2 wt%)	507	374	4400						[42]	
Al–Cu–Mg–Zn (54/22/18/6 wt%)	520	305	3140		1.51	1.13			[41]	
Al–Si–Cu (68.5/5/26.5 wt%)	525	364	2938						[42]	
Al–Cu–Sb (64.3/34/1.7 wt%)	545	331	4000						[42]	
Al–Cu (66.92/33.08 wt%)	548	372	3600						[42]	
Al–Si–Mg (83.14/11.7/5.16 wt%)	555	485	2500						[42]	
Al–Si (87.76/12.24 wt%)	557	498	2540						[42]	
Al–Si–Cu (46.3/4.6/49.1 wt%)	571	406	5560						[42]	
Al–Si–Cu (65/5/30 wt%)	571	422	2730		1.30	1.20			[41]	
Al–Si–Sb (86.4/9.6/4.2 wt%)	575	471	2700						[42]	
Al–Si (12/86 wt%)	576	560	2700		1.038	1.741	160		[44]	
Al–Si (20/80 wt%)	585	460							[44]	
Zn–Cu–Mg (49/45/6 wt%)	703	176	8670		0.42				[41]	
Cu–P (91/9 wt%)	715	134	5600						[41]	
Cu–Zn–P (69/17/14 wt%)	720	368	7000						[41]	
Cu–Zn–Si (74/19/7 wt%)	765	125	7170						[41]	
Cu–Si–Mg (56/27/17 wt%)	770	420	4150		0.75				[41]	
Mg–Ca (84/16 wt%)	790	272	1380						[41]	
Mg–Si–Zn (47/38/15 wt%)	800	314							[41]	
Cu–Si (80/20 wt%)	803	197	6600		0.50				[41]	
Cu–P–Si (83/10/7 wt%)	840	92	6880						[41]	
Si–Mg–Ca (49/30/21 wt%)	865	305	2250						[41]	
Si–Mg (56/44 wt%)	946	757	1900		0.79				[41]	

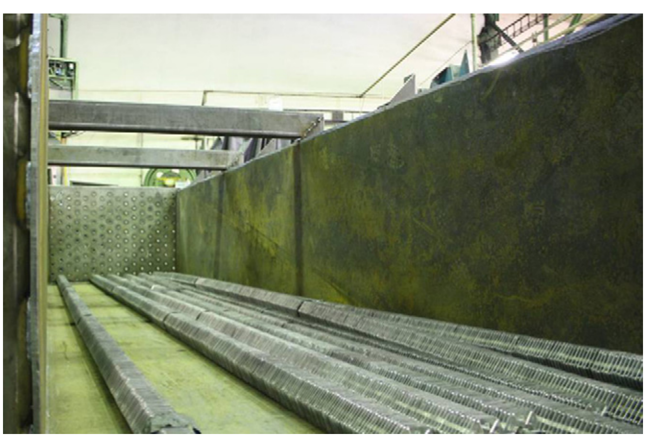


Fig. 5. PCM test module during assembly [39].

further testing in an electric heater. Sun et al. [44] tested the thermal reliability of metal alloy Al–Mg–Zn with 59.36% Al, 34.02% Mg and 6.62% Zn (wt%). DSC results showed that the melting temperature and the latent heat of fusion of the alloy decreased by 3.06–5.3 K and 10.98% respectively after 1000 thermal cycles.

4. Methods of performance enhancement

During the discharging process, the energy released by solidification of the PCM must be transported from the solid–liquid interface through the growing solid layer to the heat exchanger surface. Hence, the heat transfer coefficient is dominated by the thermal conductivity of the solid PCM. However, most PCMs usually provide low thermal conductivity around 0.5 $W\,m^{-1}\,K$), which results in poor heat transfer between the HTF and the storage material. Therefore, the design of a cost effective phase change thermal storage system requires the development of proper thermal performance enhancement technique. Based on the literature on high temperature phase change storage systems, the following techniques (as presented in Fig. 6) have been employed to enhance the thermal performance of the storage system: increasing the thermal conductivity of the PCM by compositing high conductive materials, extending heat transfer surfaces by fins and capsules, using intermediate heat transfer medium or heat pipes and employing multiple PCMs.

4.1. Enhancement using high conductive materials

The heat transfer within a PCM storage system can be enhanced by composing high thermal conducting material (sensible heat phase) into the PCM (latent heat phase). In the PCM/ceramic compound, the molten PCM is retained and immobilized within the micro-porosity defined by the ceramic network by capillary forces and surface tension, which offers the potential of using direct contact heat exchange [45,46]. Petri et al. [45] tested a packed-bed laboratory scale storage unit containing 1.22 kg composite Na_2CO_3–$BaCO_3$ (melting point of 700 °C)/MgO. The composite has been pressed into cylindrical pellets with a diameter of 2 cm

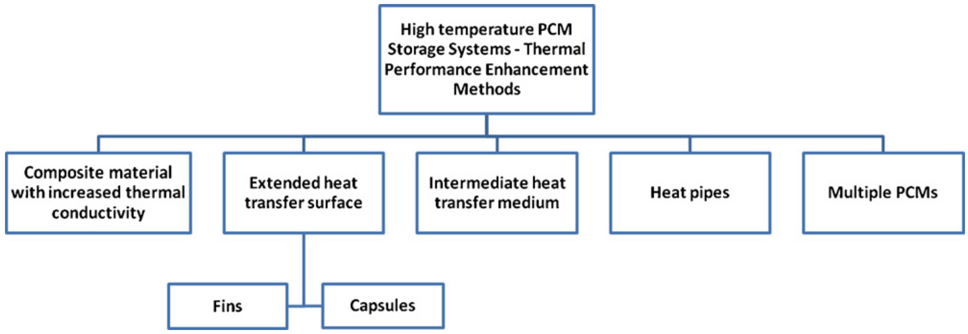


Fig. 6. Classification of investigated performance enhancement techniques in PCM-storage systems.

and a height of 1.5 cm. The 200 cycling tests demonstrated the good stability of Na_2CO_3–$BaCO_3$/MgO composite. Gokon et al. [47] experimentally examined the feasibility of using carbonate (Na_2CO_3–K_2CO_3–Li_2CO_3)/MgO composite material as a thermal storage medium to prolong the cooling time in a double-walled reactor.

Recently, graphite has been studied extensively as a heat transfer enhancer due to its high thermal conductivity, low density and chemical resistance [22,48–51]. The thermal conductivity of paraffin graphite composite can be increased up to 70 $W m^{-1} K^{-1}$ depending on the graphite percentage. The effect of mass fraction of the expanded graphite on the effective thermal conductivity of the composite is significant as presented in Fig. 7. As the cost of the material will be increased and the volume storage capacity will be reduced by the increased fraction of the graphite, the graphite content should be limited [52].

The PCM graphite composite can be obtained by infiltration/impregnation of PCM within a porous structure of graphite, dispersion of graphite mechanically within the PCM or compression of the pre-mixed graphite and PCM [53]. do Couto Aktay et al. [54] measured the effective thermal conductivity of composites based on high melting point PCM and expanded graphite. The results indicated that the effective thermal conductivity of dispersed composites depends on the thermal conductivity of graphite and are less influenced by changes in the properties of the PCM. However, the thermal conductivity of compressed composites is affected by melting/solidification cycling [54]. Generally, compression is much more effective to enhance the heat transfer than dispersion. Another advantage of compression is that the composite material can be machined into any shape e.g. by injection molding [22]. Fig. 8 shows a single segment composite material made of $NaNO_3$/KNO_3 (50/50 mol%) and expanded graphite developed with the European project DISTOR [55]. The storage unit is assembled from segments made of composite material. Holes are intended for steam pipes for the application of direct steam generation. There are numerous types of commercially available graphites, such as natural graphite flakes, expanded natural graphite and ground expanded natural graphite. Due to their respective structures and properties, different graphite types induce different conductivity enhancement to the obtained composites [51].

Bauer et al. [49] examined five $NaNO_3$/KNO_3 (50/50 mol%)/graphite composites using three different graphite types with a fraction of 5–30%. The thermal conductivity measurement by laser flash technique showed the enhancement of the thermal conductivity is in the range from 3 to 30 $W m^{-1} K^{-1}$ and the dispersion using compressed expanded graphite plate is the most effective with a small graphite fraction. Pincemin et al. [51] investigated composites made of inorganic salts/salt eutectics and graphite with various types, flake sizes and fractions by dispersion method. The salts/salt eutectics include $NaNO_3$, KNO_3, $NaNO_3$/KNO_3 (50/50 mol%), NaOH, KOH, $ZnCl_2$ and $ZnCl_2$/KCl (31.9/68.1 mol%). Thermal conductivities of salts/eutectics graphite composites at room temperature are shown in Fig. 9. The thermal conductivity of the composite was found to increase with increasing percentage of graphite. The 200 thermal cycling tests on $NaNO_3$/KNO_3 graphite composite indicated that there is no segregation of the two components but the latent heats are lowered by the presence of graphite. Also, lower graphite size leads

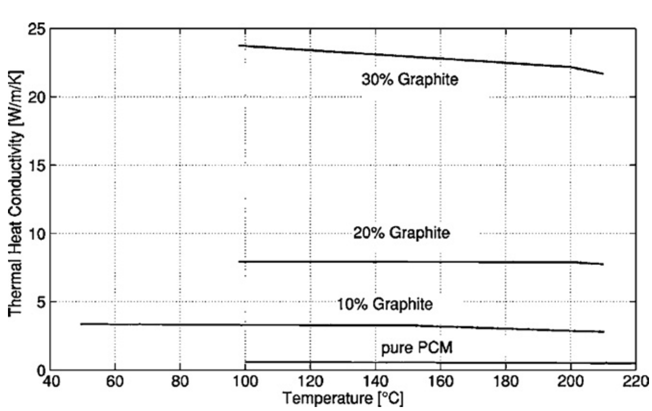


Fig. 7. The effect of mass fraction of the expanded graphite on the effective thermal conductivity of the PCM graphite composite [52].

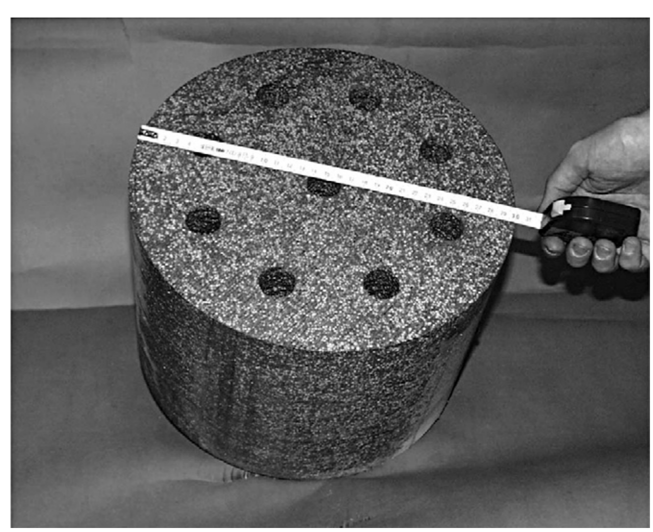


Fig. 8. Single segment made of PCM/composite material used for laboratory scale testing [55].

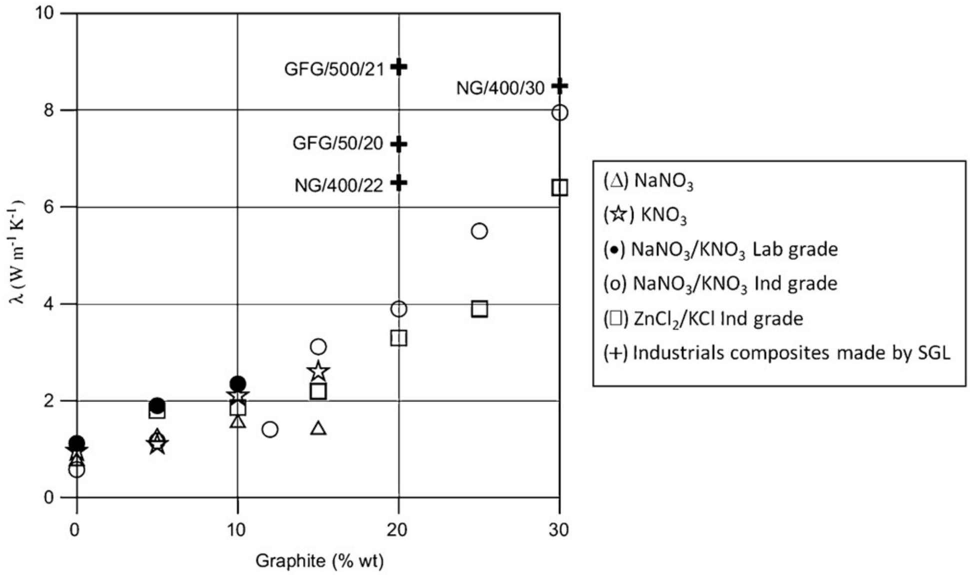


Fig. 9. Thermal conductivities of salts/eutectics graphite composites at room temperature. [51].

to a larger storage capacity after thermal cycling. At increasing temperature, the thermal conductivity of the composite was found to decrease as presented in Fig. 10. However, the salt/graphite composite usually melts over a temperature range instead of at constant temperature in the first or first several cycles and starts to behave stable afterwards [50].

Zhao and Wu [56] and Wu and Zhao [57] experimentally investigated the feasibility of using metal foam and expanded graphite to enhance the heat transfer capability of $NaNO_3$. The results showed that the heat transfer rate can be increased in both charging and discharging periods using these porous materials. Especially in the heating process of the solid $NaNO_3$, the heat transfer rate can be enhanced by 2.5 times compared to that of the pure $NaNO_3$. However, the heat transfer performance of composites is worse than that of the pure $NaNO_3$ in liquid phase as the natural convection is weakened by the porous structures.

4.2. Enhancement using extended heat transfer surface

Extension of heat transfer surface using either capsules or finned tubes will reduce the distance for heat transport within the PCM thus improving the heat transfer. Flexible capsules, usually plastic, are used for low temperature PCM applications. To encapsulate the PCMs with melting temperature above 200 °C, the material is generally expensive. If the stiff capsule is used to contain the PCM, the initial PCM volume should not exceed 80% in order to withstand the pressure variation during the melting/solidification cycling [52]. Fig. 11 shows a series of parallel cylindrical capsules with a length of 0.5 m. They are filled with eutectic $NaNO_3$–KNO_3 and integrated into a vessel [52].

Fins arranged orthogonal to the axis of the heat transfer fluid pipes, namely sandwich design as presented in Fig. 12, are generally used to improve the heat transfer in high temperature phase change

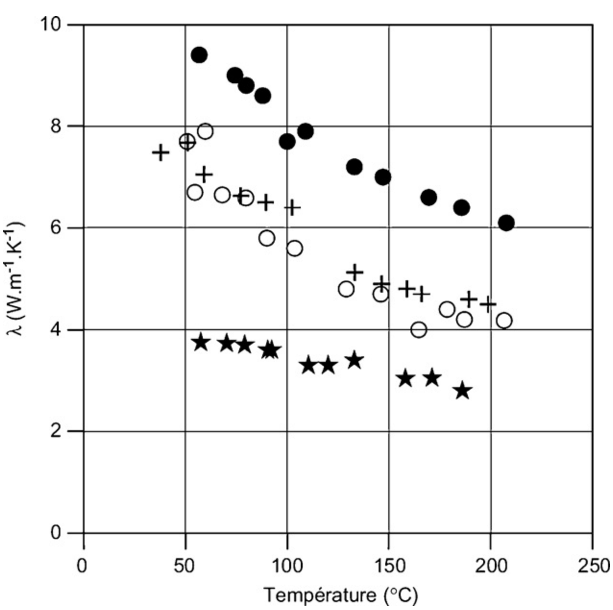


Fig. 10. Thermal conductivity of 4 types of $NaNO_3$/KNO_3–graphite composites against temperature [51].

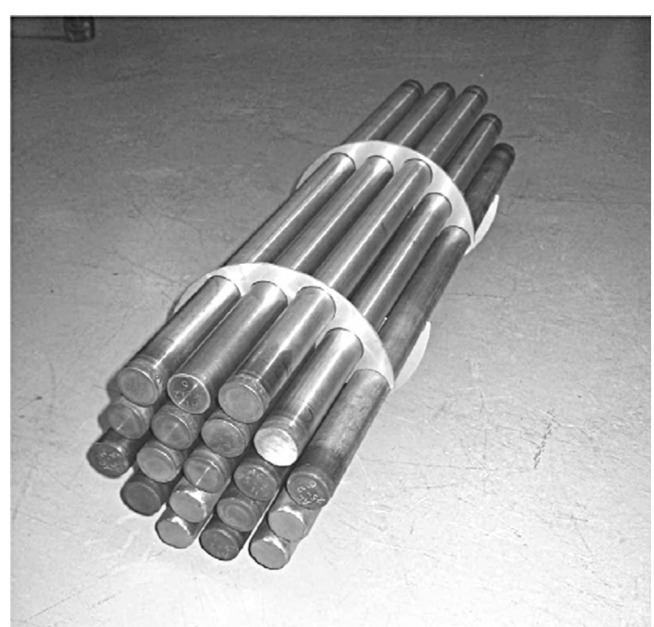


Fig. 11. Cylindrical capsules used for laboratory scale test [52].

Table 5
Properties of materials considered for fins [40].

	Graphite foil	Aluminium	Stainless steel	Carbon steel	Copper
Thermal conductivity ($W m^{-1} K^{-1}$)	150	200	20	30	350
Density (kg/m^3)	1000	2700	7800	7800	8800
Estimated volume specific cost ($\$ m^{-3}$)	10,000	7000	20,000	15,000	40,000

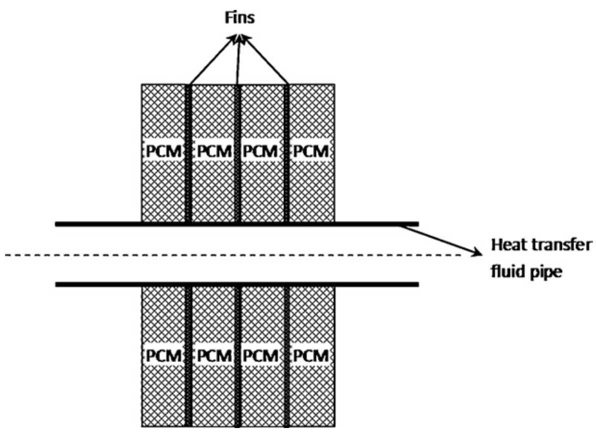


Fig. 12. Arrangement of extending heat transfer area by using fins.

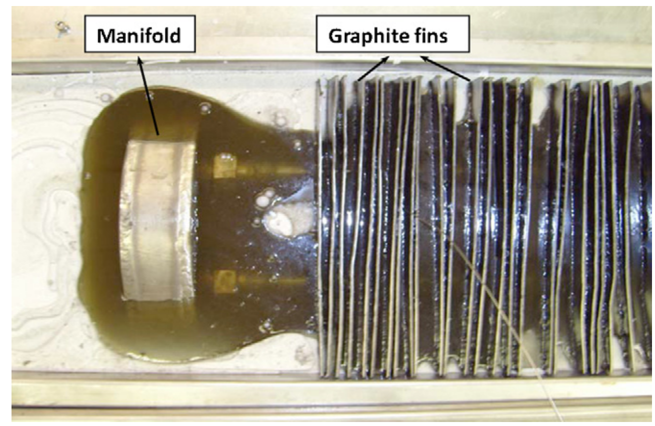


Fig. 13. A storage unit with graphite foil fins and eutectic salts as PCM [58].

storage units. The fin material can be graphite foil, aluminium, steel and copper. Table 5 shows the relevant properties and costs for various materials [58]. Volume specific cost is a quantity estimated by cost ($\$ kg^{-1}$), density ($kg/m^3$) and thermal conductivity ($W m^{-1} K^{-1}$). Due to the advantages provided by graphite foil, such as high thermal conductivity, low density and good corrosion resistivity against nitrate and nitrite salts at temperatures up to 250 °C, it has been experimentally demonstrated as fin material (Fig. 13). A sandwich configuration storage prototype was constructed and tested under real conditions. The sketch in Fig. 14 shows a top-view of the prototype (a) and a side-view of the core (b) [59]. The conductive fins are 490 mm × 490 mm 1 mm thick expanded graphite foil spaced 10 mm apart. 2100 kg of PCM (eutectic $KNO_3/NaNO_3$) with a maximum delivery latent heat of 58 kW was filled between the fins.

Aluminium fins are applicable for temperatures up to 330 °C. It has been proven to have no degradation after 400 h testing with $NaNO_3$ as a PCM [58]. Both graphite foil and aluminium show no galvanic corrosion in contact with steel since the pipe is generally made of steel. As shown in Fig. 15 [38], in order to have the same heat transport performance, fins made of steel demand much more volume than those made of graphite foil. Therefore, the cost for steel fins is significantly higher.

4.3. Enhancement using intermediate heat transfer medium

The concept of heat storage incorporating with intermediate high conductive fluid is shown in Fig. 16 [60], which is named

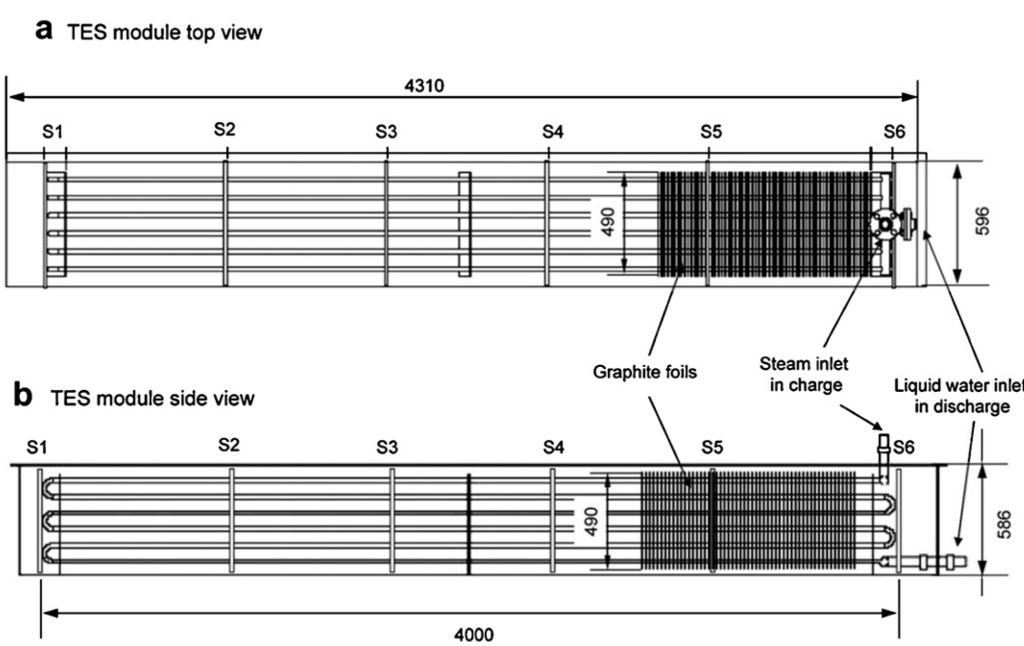


Fig. 14. Sketch of storage prototype dimensions: (a) top-view and (b) side view (all dimensions are given in mm) [59].

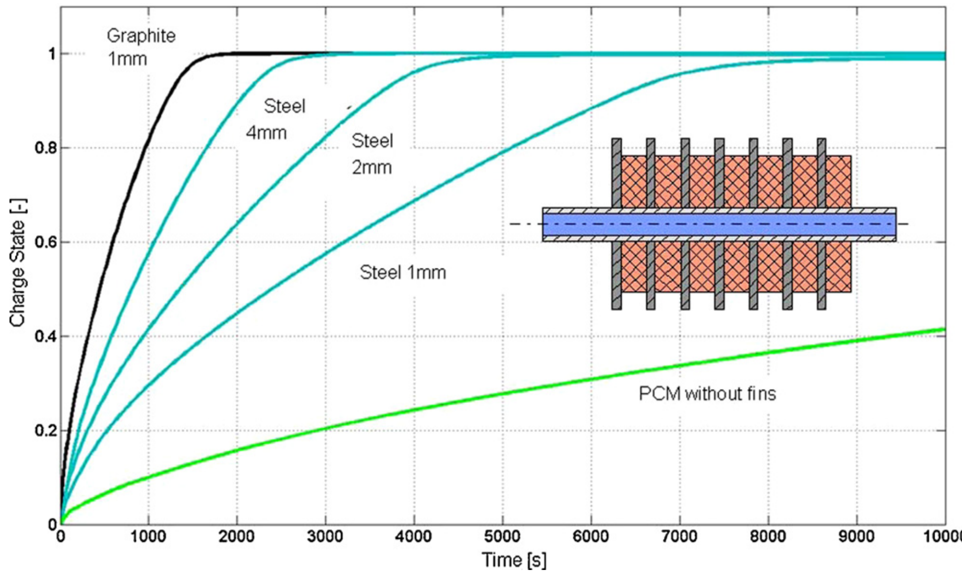


Fig. 15. Comparison of change state for PCM with our fins, with steel fins of various thicknesses and with graphite fin [38].

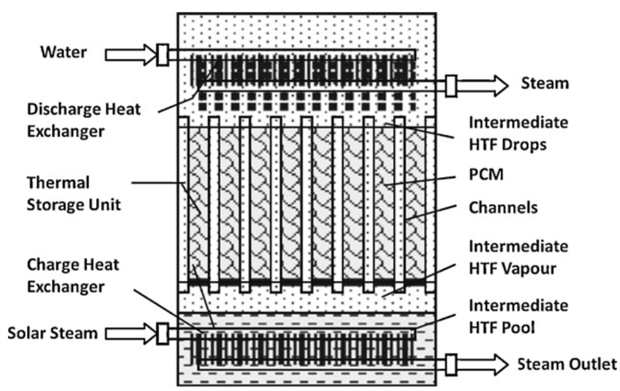


Fig. 16. Schematic diagram of the reflux heat transfer storage concept [60].

reflux heat transfer storage. The concept is based on the reflux evaporation–condensation occurring in the intermediate HTF. The whole storage system consists of a PCM storage unit, discharge and charge heat exchangers placed externally of the PCM at the top and the bottom of the storage unit. The charge heat exchanger is immersed in the liquid intermediate HTF. In the charging process, the liquid HTF absorb energy through vaporization and the vapour flows upwards through the transport channels distributed in the PCM. Then the vapour condenses on the channel's surfaces and the latent heat of vapour is transferred across the walls to the PCM. The liquefied HTF returns to the pool due to gravity. In the discharging process, the hot PCM causes the liquid HTF to evaporate and the vapour transfers energy to the working fluid passing through the top heat exchanger.

This concept was first successfully demonstrated by Adinberg et al. [61]. In the experiment, they used sodium chloride as the PCM and sodium metal as the intermediate heat transfer medium for a storage temperature of 800 °C. A metal alloy Zinc/Tin (70/30 wt%) and the eutectic mixture of biphenyl and diphenyl oxide was experimentally investigated as the PCM-HTF system for producing high-temperature superheated steam in the temperature range of 350–400 °C [60].

4.4. Enhancement using heat pipes

It is well known that heat pipes have high effective thermal conductivity. They can be incorporated into phase change thermal storage systems to serve as thermal conduits between the HTF and the PCM. Fig. 17 presents a phase change thermal storage system using heat pipes to improve the heat transfer. The heat pipes can

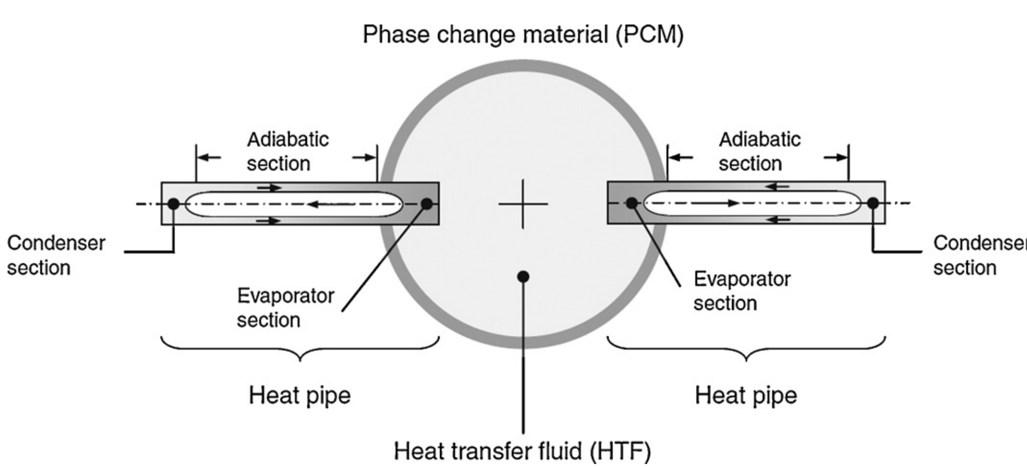


Fig. 17. Heat transfer between the PCM and the HTF using heat pipes [62].

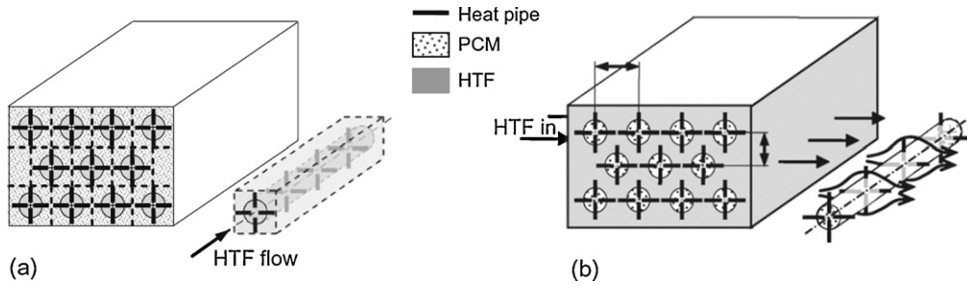


Fig. 18. Two phase change thermal storage systems: (a) the PCM surrounds the HTF tubes; (b) the HTF passes over tubes containing PCM [62].

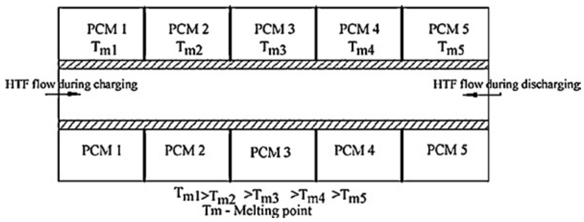


Fig. 19. Sequence of multiple PCMs in shell and tube latent heat storage unit [63].

transfer heat between the HTF and the PCM with evaporation and condensation of the heat pipe working fluid occurring at the ends of the heat pipes. Shabgard et al. [62] investigated the impact of the number of heat pipes as well as their orientation relative to the HTF flow direction and the gravity vector in two distinct system configurations as shown in Fig. 18. The prediction results indicated that the thermal performance of system (a) can exceed that of system (b) with use of fewer heat pipes.

4.5. Enhancement using multiple PCMs

Thermal storage systems employing multiple PCMs of different melting temperatures is another attractive heat transfer enhancement technology. In this type of system, a few modules containing different PCMs and different melting temperatures are connected to each other in series. When employing multiple PCMs to enhance the thermal performance of latent storage systems, it is important to select the appropriate PCMs and relative proportions of the PCMs. The multiple PCMs in shell and tube units should be in the flow direction that the melting temperature decreases in the charging process and increases in the discharging process as illustrated in Fig. 19 [63]. The heat transfer rate in the storage unit is mainly dependent on the temperature difference between the HTF and the PCM. If a single PCM is used, this temperature difference obviously decreases in the HTF flow direction, which results in decreasing heat transfer rate. If multiple PCMs are contained in the storage unit in the sequence as shown in Fig. 19, the temperature difference can be maintained to roughly constant as both the HTF temperature and the melting point of the PCM decrease in the HTF flow direction in the charging process and both of them increase in the HTF flow direction in the discharging process. Therefore, the heat flux from the PCM to the HTF is nearly constant.

In the case that the encapsulated PCM is immersed in a large storage tank so that the temperature variation of the HTF can be ignored along the flow direction, in order to extract maximum benefit, the multiple PCMs should be arranged in the radial direction rather than in the axial direction (flow direction) [63]. Wang et al. [64] experimentally investigated the melting process of a cylindrical heat storage capsule filled with three PCMs with the lowest melting point PCM at the centre and other PCMs arranged in the order of increasing melting point from the centre to the outer as presented in Fig. 20. The thermal performance of a same capsule

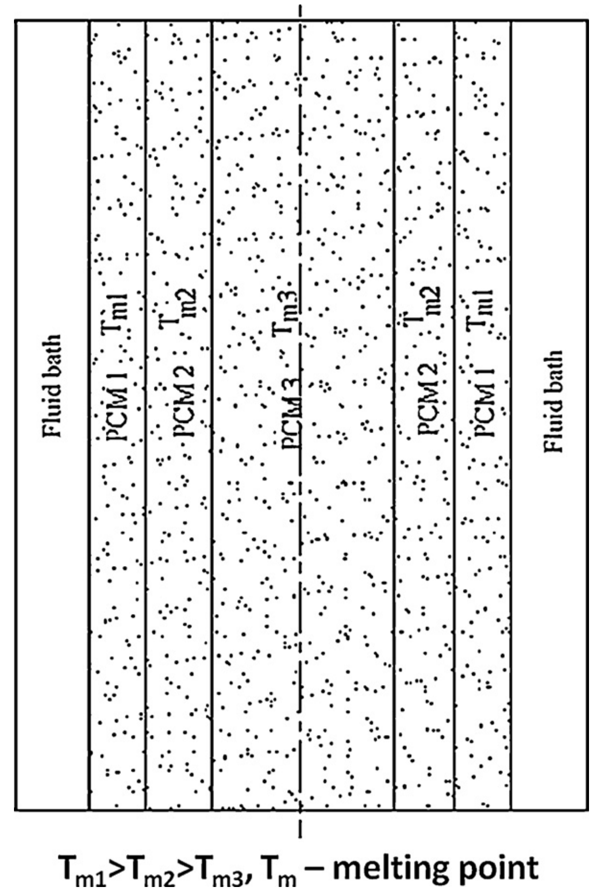


Fig. 20. Multiple PCMs in a thermal storage unit of coaxial cylindrical tubes [64].

filled with only PCM2 was also evaluated for the purpose of comparison. The results showed that the melting time was 37–42% shorter in the three PCMs capsule than that in the single PCM capsule.

Farid and Kanzawa [65] and Farid et al. [66] proposed and evaluated the thermal performance of a thermal storage system using three PCMs which were filled in a number of cylindrical capsules with air flowing across them. The results indicated that there is around 10% increase in the heat transfer rate during both the charging and discharging processes compared with the unit containing only one PCM. A similar conclusion was obtained by Adine and El Qarnia's from their research [67]. Adebiyi et al. [68] found that the efficiency of a packed bed thermal storage system employing five PCMs is 13–26% higher than that of single PCM system. Michels and Pitz-Paal [69] designed and tested a vertical shell and tube heat storage system filled with three high temperature PCMs–KNO_3 (PCM1), eutectic KNO_3/KCl (PCM2) and $NaNO_3$ (PCM3). This system corresponds to the one used for parabolic trough solar power plants. Fig. 21 shows the schematic diagram

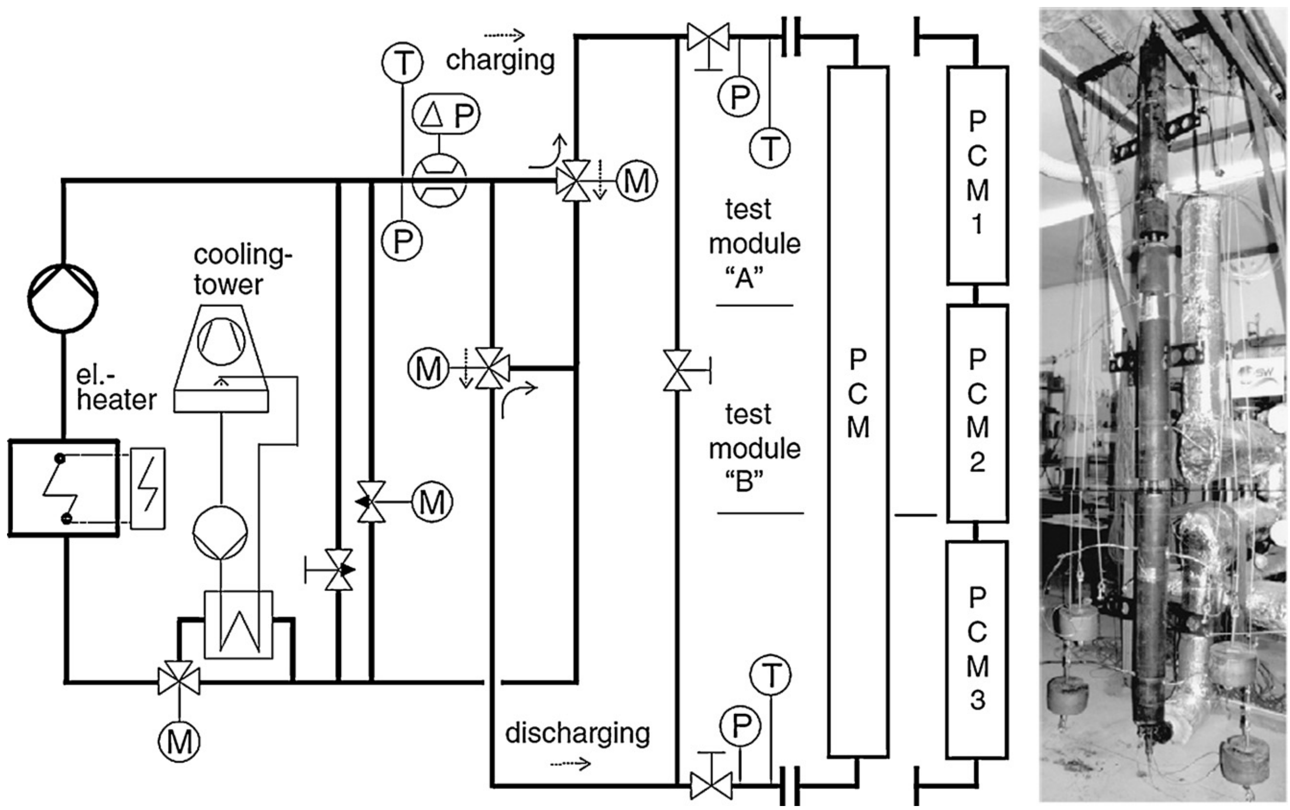


Fig. 21. Schematic diagram of experimental set up and a picture of multiple PCM storage system [69].

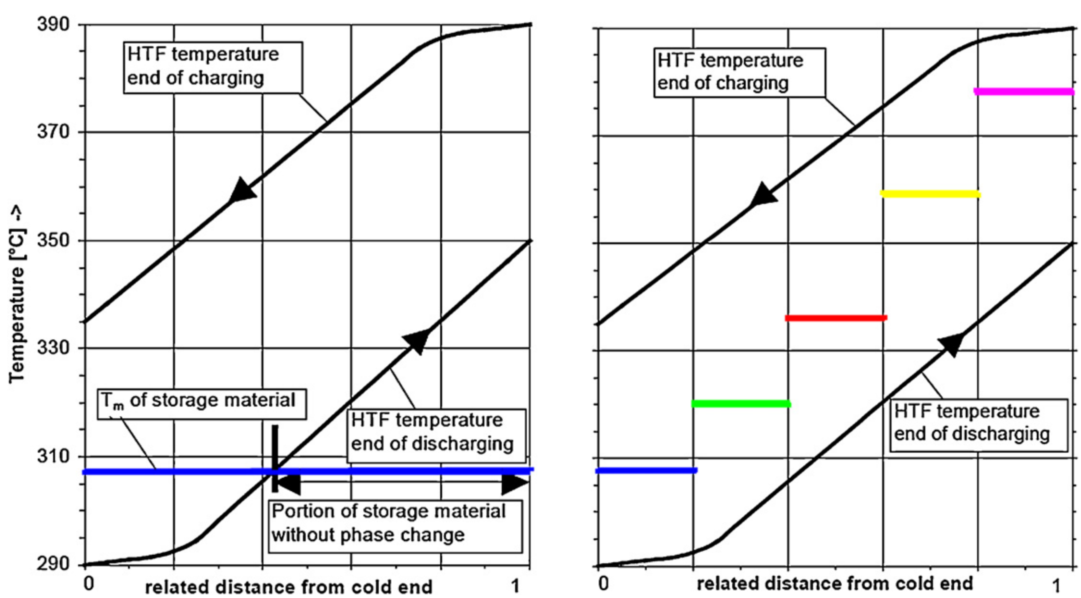


Fig. 22. Theoretical temperature distribution in a single PCM-storage system and a five PCM-storage system with staged melting temperatures [27].

of the experimental setup and a picture of multiple-PCM thermal storage unit. The experimental results showed that around 92% of the PCM in the multiple-PCM storage unit was completely molten at the end of charging and around 67% was completely solidified at the end of discharging. In the single storage unit containing $NaNO_3$ as the PCM, almost 100% of the PCM was completely molten at the end of charging but only 2% was completely solidified at end of discharging. Michels and Hahne [70] explained the reason that multiple-PCM storage unit offers a higher utilization of the possible phase change by means of Fig. 22. Also, a multiple-PCM storage unit offers a more uniform HTF outlet temperature [69,71] and higher exergy efficiency [72,73].

5. Conclusions and discussions

This paper reviews energy storage systems used in existing solar thermal power plants and proposed for future plants to be constructed. A majority of parabolic trough solar power plants have two-tank active indirect storage systems with molten salts as the storage media and synthetic oil as the HTF. The upper temperature

limit of synthetic oil restricts the solar field temperature to below 400 °C. Solar tower power plants can achieve high working temperatures, which potentially allow for reduced storage cost and better power cycle efficiency.

High temperature PCMs with melting temperatures above 300 °C are reviewed. The promising substances include pure inorganic salts, salt eutectics, metals and metallic eutectic alloys. Most of the pure inorganic salts and salt eutectics included are on the basis of chlorides, nitrates and carbonates which have low cost. The following detailed conclusions can be drawn based on the literature review:

- There are five pure inorganic salts based on nitrates and hydroxides having melting temperatures in the range of 300–550 °C, the latent heats of fusion of which are between 95 and 172 kJ kg^{-1}. The value is below half that of water's heat of fusion. Compared with nitrate and hydroxide salts, chloride and carbonate salts have a higher melting temperature (above 700 °C) and higher latent heat of fusion (above 200 kJ kg^{-1}). The latent heats of fusion of some chloride salts ($MgCl_2$, KCl and NaCl) are even above 350 kJ kg^{-1}.
- More potential PCMs with melting temperatures in the range of 300–550 °C lie in binary and ternary chloride eutectic salts. They also offer high latent heat of fusion, most of which are above 250 kJ kg^{-1}. The heat of fusion of eutectic salt $MgCl_2$/KCl even reaches 430 kJ kg^{-1}.
- $NaNO_3$ is the most investigated latent heat storage medium, as the melting temperature suits steam generation at a pressure of around 100 bar in direct steam generating power plants.
- Metal and metal alloys have many advantages, such as high thermal conductivity, low corrosion activity, small volume change during melting/freezing and no supercooling. Therefore, they are better than inorganic salts in some cases, but they cost much higher than the chloride, nitrate and carbonate salts and salt eutectics in Tables 2 and 3.
- Among the reviewed PCMs, only pure salt $NaNO_3$, ternary carbonate eutectic salt $Li_2CO_3/K_2CO_3/Na_2CO_3$ and metal alloy Al/Mg/Zn have been cycle tested, having undergone 172, 50 and 1000 thermal cycles respectively.

Identifying a suitable PCM is one aspect in the development of a high temperature phase change thermal storage system. Another aspect and also a challenge is to improve the thermal performance of the system due to the low thermal conductivity of most salts. This paper reviews the thermal performance enhancement methods employed in high temperature phase change thermal storage systems as follows:

- Increasing the thermal conductivity of the PCM by adding high conductive materials. Graphite has been widely investigated by researchers so far. The thermal conductivity of the PCM graphite composite is dependent on the mass faction of graphite, graphite type, particle size and manufacturing method. Generally, the thermal conductivity of the composite increases as the increasing mass faction of graphite, but at the same time, the cost will be increased and the volume storage capacity will be reduced. Therefore, the mass fraction of graphite in the composite should not be over 20%.
- Extending heat transfer surface by fins and capsules. Encapsulating the high temperature PCMs is usually expensive due to the high cost of capsule material. Sandwich configuration with graphite foil fins (up to 250 °C) or aluminium fins (330 °C) has proven to be promising to construct high temperature phase change thermal storage systems.
- Employing multiple PCMs. Packing the phase change thermal storage system with multiple PCMs of different melting temperatures is capable of increasing the thermal performance of the storage system compared with using a single PCM. However, attention needs to be paid on selecting proper PCMs and the relative proportions of each PCM.
- Using intermediate heat transfer medium or heat pipes. Due to the complexity of the system configuration, those techniques are still under research and there are only a limited numbers of references on those techniques.

Acknowledgement

This project has been supported by the Australian Government through the Australian Solar Institute (ASI), part of the Clean Energy Initiative. The Australian Government, through the ASI, is supporting Australian research and development in solar photovoltaic and solar thermal technologies to help solar power become cost competitive with other energy sources.

References

[1] Gil A, Medrano M, Martorell I, Lázaro A, Dolado P, Zalba B, et al. State of the art on high temperature thermal energy storage for power generation. Part 1 – concepts, materials and modellization. Renewable and Sustainable Energy Reviews 2010;14:31–55.
[2] Morrison DJ, Abdel-Khalik SI. Effects of phase-change energy storage on the performance of air-based and liquid-based solar heating systems. Solar Energy 1978;20:57–67.
[3] Das S, Dutta TK. Mathematical modeling and experimental studies on solar energy storage in a phase change material. Solar Energy 1993;51:305–12.
[4] Kaygusuz Kl. Phase change energy storage for solar heating systems, Energy Sources, Part A: Recovery. Utilization, and Environmental Effects 2003;25: 791–807.
[5] Saman W, Bruno F, Halawa E. Thermal performance of PCM thermal storage unit for a roof integrated solar heating system. Solar Energy 2005;78:341–9.
[6] Mehling H, Hiebler S, Schweigler C, Keil C, Helm M. Test results from a latent heat storage developed for a solar heating and cooling system. In: EUROSUN 2008 – 1st international conference on solar heat, cooling and buildings. 2008.
[7] Vakilaltojjar SM. Phase change thermal storage system for space heating and cooling, Doctor of Philosophy Thesis, University of South Australia, Adelaide, Australia, 2000, p. 217.
[8] Vakilaltojjar SM, Saman W. Analysis and modelling of a phase change storage system for air conditioning applications. Applied Thermal Engineering 2001;21:249–63.
[9] Hed G, Bellander R. Mathematical modelling of PCM air heat exchanger. Energy and Buildings 2006;38:82–9.
[10] Liu M, Saman W, Bruno F. Validation of a mathematical model for encapsulated phase change material flat slabs for cooling applications. Applied Thermal Engineering 2011;31:2340–7.
[11] Farid M, Kong W. Underfloor heating with latent heat storage, Proceedings of the Institution of Mechanical Engineers, Part A. Journal of Power and Energy 2001;215:601–9.
[12] Lin K, Zhang Y, Xu X, Di H, Yang R, Qin P. Experimental study of under-floor electric heating system with shape-stabilized PCM plates. Energy and Buildings 2005;37:215–20.
[13] Nagano K, Takeda S, Mochida T, Shimakura K, Nakamura T. Study of a floor supply air conditioning system using granular phase change material to augment building mass thermal storage – heat response in small scale experiments. Energy and Buildings 2006;38:436–46.
[14] Scalat S, Banu D, Hawes D, Parish J, Haghighata F, Feldman D. Full scale thermal testing of latent heat storage in wallboard. Solar Energy Materials and Solar Cells 1996;44:49–61.
[15] Lv S, Feng G, Zhu N, Dongyan L. Experimental study and evaluation of latent heat storage in phase change materials wallboards. Energy and Buildings 2007;39:1088–91.
[16] Zhou G, Yang Y, Wang X, Zhou S. Numerical analysis of effect of shape-stabilized phase change material plates in a building combined with night ventilation. Applied Energy 2009;86:52–9.
[17] Sharma SD, Iwata T, Kitano H, Sagara K. Thermal performance of a solar cooker based on an evacuated tube solar collector with a PCM storage unit. Solar Energy 2005;78:416–26.
[18] Muthusivagami RM, Velraj R, Sethumadhavan R. Solar cookers with and without thermal storage – a review. Renewable and Sustainable Energy Reviews 2010;14:691–701.
[19] El-Sebaii AA, Al-Heniti S, Al-Agel F, Al-Ghamdi AA, Al-Marzouki F. One thousand thermal cycles of magnesium chloride hexahydrate as a promising PCM for indoor solar cooking. Energy Conversion and Management 2011;52:1771–7.
[20] Abhat A. Low temperature latent heat thermal energy storage: heat storage materials. Solar Energy 1983;30:313–32.

[21] Zalba B, Marín JM, Cabeza LF, Mehling H. Review on thermal energy storage with phase change: materials, heat transfer analysis and applications. Applied Thermal Engineering 2003;23:251–83.
[22] Mehling H, Cabeza LF. Heat and cold storage with PCM – an up to date introduction into basics and applications. Berlin, Germany: Springer; 2008.
[23] Kenisarin M, Mahkamov K. Solar energy storage using phase change materials. Renewable and Sustainable Energy Reviews 2007;11:1913–65.
[24] Herrmann U, Kearney DW. Survey of thermal energy storage for parabolic trough power plants. Journal of Solar Energy Engineering 2002;124:145–52.
[25] Lane GA. Solar heat storage: latent heat material, vol. I: background and scientific principles. Florida: CRC Press; 1983.
[26] Medrano M, Gil A, Martorell I, Potau X, Cabeza LF. State of the art on high-temperature thermal energy storage for power generation. Part 2 – case studies. Renewable and Sustainable Energy Reviews 2010;14:56–72.
[27] Pilkington Solar International GmbH.Survey of thermal storage for parabolic trough power plants. 2000.
[28] Kenisarin MM. High-temperature phase change materials for thermal energy storage. Renewable and Sustainable Energy Reviews 2010;14:955–70.
[29] Hoshi A, Mills DR, Bittar A, Saitoh TS. Screening of high melting point phase change materials (PCM) in solar thermal concentrating technology based on CLFR. Solar Energy 2005;79:332–9.
[30] Elgafy A, Mesalhy O, Lafdi K, Numerical. Experimental investigations of melting and solidification processes of high melting point PCM in a cylindrical enclosure. Journal of Heat Transfer 2004;126:869–75.
[31] Nomura T, Oya T, Okinaka N, Akiyama T. Feasibility of an advanced waste heat transportation system using high-temperature phase change material (PCM). ISIJ International 2010;50:1326–32.
[32] Nomura T, Okinaka N, Akiyama T. Waste heat transportation system, using phase change material (PCM) from steelworks to chemical plant. Resources, Conservation and Recycling 2010;54:1000–6.
[33] Shin BC, Kim SD, Park W-H. Ternary carbonate eutectic (lithium, sodium and potassium carbonates) for latent heat storage medium. Solar Energy Materials 1990;21:81–90.
[34] Ponnappan R, Jacobson DL. Performance of a cylindrical phase change thermal energy storage unit. In: American Institute of Aeronautics and Astronautics, aerospace sciences meeting. 1982.
[35] Xing Y-M, Xu X, Yuan X-g, Cui H-T, Zhang Y-h. Numerical simulation of high-temperature phase change heat storage system. Heat Transfer—Asian Research 2004;33:32–41.
[36] Hall CA, Glakpe EK, Cannon JN. Modeling cyclic phase change and energy storage in solar heat receivers. In: 32nd Thermophysics conference. 1997.
[37] Bauer T, Laing D, Kroner U, Tamme R. Sodium nitrate for high temperature latent heat storage. In: The 11th international conference on thermal energy storage. 2009.
[38] Laing D, Bauer T, Steinmann W-D, Lehmann D. Advanced high temperature latent heat storage system – design and test results. In: The 11th international conference on thermal energy storage. 2009.
[39] Laing D, Bahl C, Bauer T, Lehmann D, Steinmann W-D. Thermal energy storage for direct steam generation. Solar Energy 2011;85:627–33.
[40] Farkas D, Birchenall C. New eutectic alloys and their heats of transformation. Metallurgical and Materials Transactions A 1985;16:323–8.
[41] Gasanealiev AM, Gamataeva BY. ChemInform abstract: heat-accumulating properties of melts. ChemInform 2000;31.
[42] Akiyama T, Ashizawa Y, Yagi J. Storage and release of heat in a single spherical capsule containing phase-change material with a high melting point. Heat transfer – Japanese research 1992;21:199–217.
[43] Wang X, Liu J, Zhang Y, Di H, Jiang Y. Experimental research on a kind of novel high temperature phase change storage heater. Energy Conversion and Management 2006;47:2211–22.
[44] Sun JQ, Zhang RY, Liu ZP, Lu GH. Thermal reliability test of Al–34%Mg–6%Zn alloy as latent heat storage material and corrosion of metal with respect to thermal cycling. Energy Conversion and Management 2007;48:619–24.
[45] Petri RJ, Ong ET, Olszewski M. High temperature composite thermal storage systems. In: 19th Intersociety energy conversion engineering conference. 1984.
[46] Tamme R, Taut U, Streuber C, Kalfa H. Energy storage development for solar thermal processes. Solar Energy Materials 1991;24:386–96.
[47] Gokon N, Nakano D, Inuta S, Kodama T. High-temperature carbonate/MgO composite materials as thermal storage media for double-walled solar reformer tubes. Solar Energy 2008;82:1145–53.
[48] Zhang P, Song L, Lu H, Wang J, Hu Y. The influence of expanded graphite on thermal properties for paraffin/high density polyethylene/chlorinated paraffin/antimony trioxide as a flame retardant phase change material. Energy Conversion and Management 2010;51:2733–7.
[49] Bauer T, Tamme R, Christ M, Őttinger O. PCM-graphite composites for high temperature thermal energy storage. In: Ecostock' 2006—10th international conference on thermal energy storage. 2006.
[50] Lopez J, Caceres G, Palomo Del Barrio E, Jomaa W. Confined melting in deformable porous media: a first attempt to explain the graphite/salt composites behaviour. International Journal of Heat and Mass Transfer 2010;53: 1195–207.
[51] Pincemin S, Olives R, Py X, Christ M. Highly conductive composites made of phase change materials and graphite for thermal storage. Solar Energy Materials and Solar Cells 2008;92:603–13.
[52] Steinmann W-D, Tamme R. Latent heat storage for solar steam systems. Journal of Solar Energy Engineering 2008;130:011004–5.
[53] Nomura T, Okinaka N, Akiyama T. Technology of latent heat storage for high temperature application: a review. ISIJ International 2010;50:1229–39.
[54] do Couto Aktay K, Tamme R, Müller-Steinhagen H. Thermal conductivity of high-temperature multicomponent materials with phase change. International Journal of Thermophysics 2008;29:678–92.
[55] Tamme R. The DISTOR Project. Consortium-objective-achievements. In: DISTOR dissemination workshop. Energy storage for direct steam solar power plants. 2007.
[56] Zhao CY, Wu ZG. Heat transfer enhancement of high temperature thermal energy storage using metal foams and expanded graphite. Solar Energy Materials and Solar Cells 2011;95:636–43.
[57] Wu ZG, Zhao CY. Experimental investigations of porous materials in high temperature thermal energy storage systems. Solar Energy 2011;85:1371–80.
[58] Steinmann W-D, Laing D, Tamme R. Development of PCM storage for process heat and power generation. Journal of Solar Energy Engineering 2009;131:041004–9.
[59] Bayón R, Rojas E, Valenzuela L, Zarza E, León J. Analysis of the experimental behaviour of a 100 kWth latent heat storage system for direct steam generation in solar thermal power plants. Applied Thermal Engineering 2010;30:2643–51.
[60] Adinberg R, Zvegilsky D, Epstein M. Heat transfer efficient thermal energy storage for steam generation. Energy Conversion and Management 2010;51:9–15.
[61] Adinberg R, Yogev A, Kaftori D. High temperature thermal energy storage an experimental study. J Phys IV France 1999;9:PR3.
[62] Shabgard H, Bergman TL, Sharifi N, Faghri A. High temperature latent heat thermal energy storage using heat pipes. International Journal of Heat and Mass Transfer 2010;53:2979–88.
[63] Jegadheeswaran S, Pohekar SD. Performance enhancement in latent heat thermal storage system: a review. Renewable and Sustainable Energy Reviews 2009;13:2225–44.
[64] Wang J, Ouyang Y, Chen G. Experimental study on charging processes of a cylindrical heat storage capsule employing multiple-phase-change materials. International Journal of Energy Research 2001;25:439–47.
[65] Farid MM, Kanzawa A. Thermal performance of a heat storage module using PCM's with different melting temperatures: mathematical modeling. Journal of Solar Energy Engineering 1989;111:152–7.
[66] Farid MM, Kim Y, Kansawa A. Thermal performance of a heat storage module using PCM's with different melting temperature: experimental. Journal of Solar Energy Engineering 1990;112:125–31.
[67] Adine HA, El Qarnia H. Numerical analysis of the thermal behaviour of a shell-and-tube heat storage unit using phase change materials. Applied Mathematical Modelling 2009;33:2132–44.
[68] Adebiyi GA, Hodge BK, Steele WG, Jalalzadeh-Azar A, Nsofor EC. Computer simulation of a high-temperature thermal energy storage system employing multiple families of phase-change storage materials. Journal of Energy Resources Technology 1996;118:102–11.
[69] Michels H, Pitz-Paal R. Cascaded latent heat storage for parabolic trough solar power plants. Solar Energy 2007;81:829–37.
[70] Michels H, Hahne E. Cascaded latent heat storage for solar thermal power stations. In: EuroSun'96. 1996.
[71] Seeniraj RV, Lakshmi Narasimhan N. Performance enhancement of a solar dynamic LHTS module having both fins and multiple PCMs. Solar Energy 2008;82:535–42.
[72] Aceves-Saborio S, Nakamura H, Reistad GM. Optimum efficiencies and phase change temperatures in latent heat storage systems. Journal of Energy Resources Technology 1994;116:79–86.
[73] Domanski R, Fellah G. Exergy analysis for the evaluation of a thermal storage system employing PCMS with different melting temperatures. Applied Thermal Engineering 1996;16:907–19.
[74] Muren R, Arias DA, Luptowski B. Performance based cost modelling of phase change thermal energy storage for high temperature concentrating solar power systems. In: ASME 2009 International Mechanical Engineering Congress & Exposition. 2009.
[75] Zarza E, Valenzuela L, León J, Hennecke K, Eck M, Weyers HD, et al. Direct steam generation in parabolic troughs: Final results and conclusions of the DISS project. Energy 2004;29:635–44.
[76] Maruoka N, Sato K, Yagi J-I, Akiyama T. Development of PCM for recovering high temperature waste heat and utilization for producing hydrogen by reforming reaction of methane. ISIJ International 2002;42:215–9.